

AD No. AD A 055467
DDC FILE COPY



CEEDO



CEEDO-TR-78-17

~~FOR FURTHER TRAN~~ *TR-1*
2

THE AUTOXIDATION OF HYDRAZINE VAPOR

DANIEL A. STONE

DET 1 CEEDO ADTC/ESC
TYNDALL AFB FL 32403

D D C
REFURBISHED
JUN 22 1978
REGRILLE
JF P

JANUARY 1978

FINAL REPORT FOR PERIOD
NOVEMBER 1975-DECEMBER 1977

Approved for public release; distribution unlimited

CIVIL AND ENVIRONMENTAL
ENGINEERING DEVELOPMENT OFFICE

(AIR FORCE SYSTEMS COMMAND)
TYNDALL AIR FORCE BASE
FLORIDA 32403

ER RE 00 00

DEPARTMENT OF THE AIR FORCE
AIR FORCE CIVIL ENGINEERING CENTER (AFESA)
TYNDALL AIR FORCE BASE FLORIDA 32403



REPLY TO 01
ATTN OF:

11 April 1978

SUBJECT: CEEDO TR 78-13, The Autoxidation of Hydrazine Vapor

TO: Det 1, ADTC/PRX

The above technical report has been cleared for public release.

FOR THE COMMANDER

John G. Terino
JOHN G. TERINO, Major, USAF
Director of Information

UNCLASSIFIED

SECURITY CLASSIFICATION OF THIS PAGE (When Data Entered)

REPORT DOCUMENTATION PAGE		READ INSTRUCTIONS BEFORE COMPLETING FORM
1. REPORT NUMBER CEEDO-TR-78-17	2. GOVT ACCESSION NO.	3. RECIPIENT'S CATALOG NUMBER
4. TITLE (and Subtitle) THE AUTOXIDATION OF HYDRAZINE VAPOR		5. TYPE OF REPORT & PERIOD COVERED FINAL REPORT Nov 1975 - Dec 1977
6. PERFORMING ORG. REPORT NUMBER		
7. AUTHOR(S) Daniel A. Stone	8. CONTRACT OR GRANT NUMBER(s)	
9. PERFORMING ORGANIZATION NAME AND ADDRESS Det 1 (CEEDO) ADTC/ECC Tyndall AFB FL 32403	10. PROGRAM ELEMENT, PROJECT, TASK AREA & WORK UNIT NUMBERS Program Element 62601F Project 19004C01	
11. CONTROLLING OFFICE NAME AND ADDRESS Det 1 (CEEDO) ADTC Tyndall AFB FL 32403	12. REPORT DATE January 1978	
14. MONITORING AGENCY NAME & ADDRESS (if different from Controlling Office) 1741 1441	13. NUMBER OF PAGES 146	
15. SECURITY CLASS. (of this report) UNCLASSIFIED		
15a. DECLASSIFICATION/DOWNGRADING SCHEDULE		
16. DISTRIBUTION STATEMENT (of this Report) Approved for public release; distribution unlimited.		
17. DISTRIBUTION STATEMENT (of the abstract entered in Block 20, if different from Report)		
18. SUPPLEMENTARY NOTES Available in DDC		
19. KEY WORDS (Continue on reverse side if necessary and identify by block number) Hydrazine Environmental Simulation Oxidation Environmental Quality Air Pollution Missile Fuels		
20. ABSTRACT (Continue on reverse side if necessary and identify by block number) Results of three studies on the ambient temperature autoxidation of hydrazine vapor are presented. These studies show that the main reaction is $N_2H_4 + O_2 = N_2 + 2H_2O$, with ammonia being produced as a side product. The rate of the main reaction, as well as the side reaction producing ammonia, is greatly influenced by the surface to volume ratio and the surface composition of the reaction vessel. Hydrazine half life varied from a few minutes to several hours depending upon experimental conditions.		

PREFACE

This report documents work performed during the period November 1975 through December 1977 under Program Element 62601F, Project 1900, Subtask 4C01. The work was initiated at Kirtland Air Force Base, New Mexico and continued at Tyndall Air Force Base, Florida. A portion of the work was co-conducted by Capt Edward R. Ricco. The author and principle investigator is Daniel A. Stone, research chemist.

The author wishes to thank Capt Ricco for his assistance in part of this study, and acknowledge him as writer of the computer program included in this report.

This report has been reviewed by the Information Officer (OI) and is releasable to the National Technical Information Service (NTIS). At NTIS it will be available to the general public, including foreign nations.

This technical report has been reviewed and is approved for publication.

Daniel A. Stone

DANIEL A. STONE
Research Chemist

Michael G. MacNaughton

MICHAEL G. MACNAUGHTON, Major, USAF, BSC
Chief, Environmental Sciences Div

Peter A. Crowley

PETER A. CROWLEY, Major, USAF, BSC
Director of Environics

Joseph S. Pizzuto

JOSEPH S. PIZZUTO, Colonel, USAF, BSC
Commander

ACCESSION NO.	112
NTIS	1978 EDITION
DOC	1978 EDITION
UNTRACED	
1.300	
BY	
DISTRIBUTION / SECURITY CODES	
Dist.	1000
Ref.	1000
Cr. SPECIAL	

78 06 08 020

TABLE OF CONTENTS

Section	Title	Page
I	INTRODUCTION	1
II	MATERIALS	2
III	OXIDATION IN A 30-ML FLASK	3
IV	OXIDATION IN A 55-LITER REACTION CELL	10
V	OXIDATION IN REACTION VESSELS OF DIFFERENT SURFACE TO VOLUME RATIOS	17
VI	CONCLUSIONS	34
	REFERENCES	36
	APPENDIX	37

LIST OF FIGURES

Figure	Title	Page
1	300-Ml Pyrex [®] Reaction Flask	4
2	GC Calibration Curve for Oxygen and Nitrogen	5
3	Long Path Reaction Cell and Peripheral Equipment	11
4	Hydrazine Calibration Curve (Long Path Cell)	13
5	Plot of Hydrazine Concentration versus Time for the 55-Liter Cell (Note: each different symbol represents a separate experimental run)	15
6	Plot of Water Concentration versus Time for the 55-Liter Cell (Note: each different symbol represents a separate experimental run)	16
7	5-Liter Pyrex [®] Reaction Vessel (Showing exploded View of Window Mounting System)	18
8	Optical Path and Vacuum Manifold System used with the 5-Liter Flask and 44 x 2 cm Cell	20
9	Hydrazine Calibration Curve (5-Liter) Flask	21
10	Ammonia Calibration Curve (44 x 2 cm Cell)	22
11	Absorption Spectra of Hydrazine, Water, and Ammonia Showing Comparative Band Positions	24
12	Plots of Hydrazine and Ammonia Concentration versus Time for the 5-Liter Flask (Uncoated)	25
13	Plots of Hydrazine and Ammonia Concentration versus Time for the 44 x 2 cm Cell	26
14	Plots of Hydrazine Concentration versus Time for the 5-Liter Flask (Paraffin Coated)	27
15	Plots of Hydrazine Concentration versus Time for the 5-Liter Flask (Paraffin Coated with Glass Tubing)	29
16	Plots of Hydrazine Concentration versus Time for the 44 x 2 cm Cell (with Teflo [®] - Tubing)	30
17	Plots of Hydrazine Concentration versus Time for the 44 x 2 cm Cell (with Glass Tubing)	31

LIST OF FIGURES (continued)

Figure	Title	Page
18	Hydrazine Oxidation Spectra Recorded in the 5-Liter Flask	32
19	Hydrazine Oxidation Spectra Recorded in the 44 x 2 cm Cell	33

SECTION I
INTRODUCTION

Hydrazine and its monomethyl and dimethyl derivatives are finding ever increasing use in the Air Force as rocket fuels and fuels for thrusters and small electrical power generating units. With this increased use comes the necessity to characterize these fuels in terms of their toxicity and environmental fate. Studies of the vapor phase oxidation of these fuels are being conducted at the CEEDO Environmental Chemistry Laboratory, Tyndall AFB, Florida.

Despite the fact that hydrazine fuels have been in use for some time, little is known about their eventual fate in the environment in cases of accidental spills or routine handling and venting operations.

Hydrazine decomposition kinetics have been extensively studied in aqueous solution (Reference 1), high temperature regions (Reference 2), and in conjunction with various catalysts (Reference 3). However, there is apparently only one study (Reference 4) where the oxidation of hydrazine vapor is considered at temperatures below 200 °C.

Air Force operations involving hydrazine are conducted almost exclusively at ambient atmospheric conditions. It is therefore essential that hydrazine oxidation be characterized under such conditions.

SECTION II
MATERIALS

In all experiments described in this report, hydrazine was used without further purification as received from either Eastman Organic Chemicals (purity 95+ percent) or from Rocky Mountain Arsenal (fuel grade, 98+ percent purity). The nitrogen gas was 99.998 percent pure and the oxygen gas 99.99 percent pure, both were from Air Products.

SECTION III
OXIDATION IN A 300-ML FLASK

EXPERIMENTAL

This phase of early work on hydrazine oxidation was carried out in a 300 ml Pyrex[®] flask equipped with a Fisher-Porter Teflon[®] vacuum valve and a silicon rubber septum. The flask is shown in Figure 1. The flask was evacuated to less than 25 millitorr then filled with a synthetic atmosphere of helium and oxygen, directly from cylinders. Pressures were measured with a Wallace-Tiernan Model FA-160230 absolute pressure gauge.

Hydrazine was added to the flask by injection through the septum with an SGE 500- μ l syringe. After adding the hydrazine, mixing was accomplished by shaking the flask (containing a few Teflon[®] chips) for 30 seconds. After this preparation, 2-cc samples were withdrawn through the septum with a Precision Sampling 10-cc gas syringe and analyzed.

The gas samples were analyzed for nitrogen and oxygen on a Gow Mac Model 69-550 gas chromatograph equipped with a Supelco 1/4 in by 4' molecular sieve 13x column and a thermal conductivity detector. GC operating conditions were: carrier gas flow 40 cc/min (helium), bridge current 150 mA, injector port temperature 25 °C, column temperature 34 °C, and detector temperature 80 °C.

The calibration curves for nitrogen and oxygen were generated by averaging the peak height times attenuation (in arbitrary units) for a series of four injections at pressures of 0, 25, 50, 75, and 100 torr. The curves were linear over this range as shown in Figure 2.

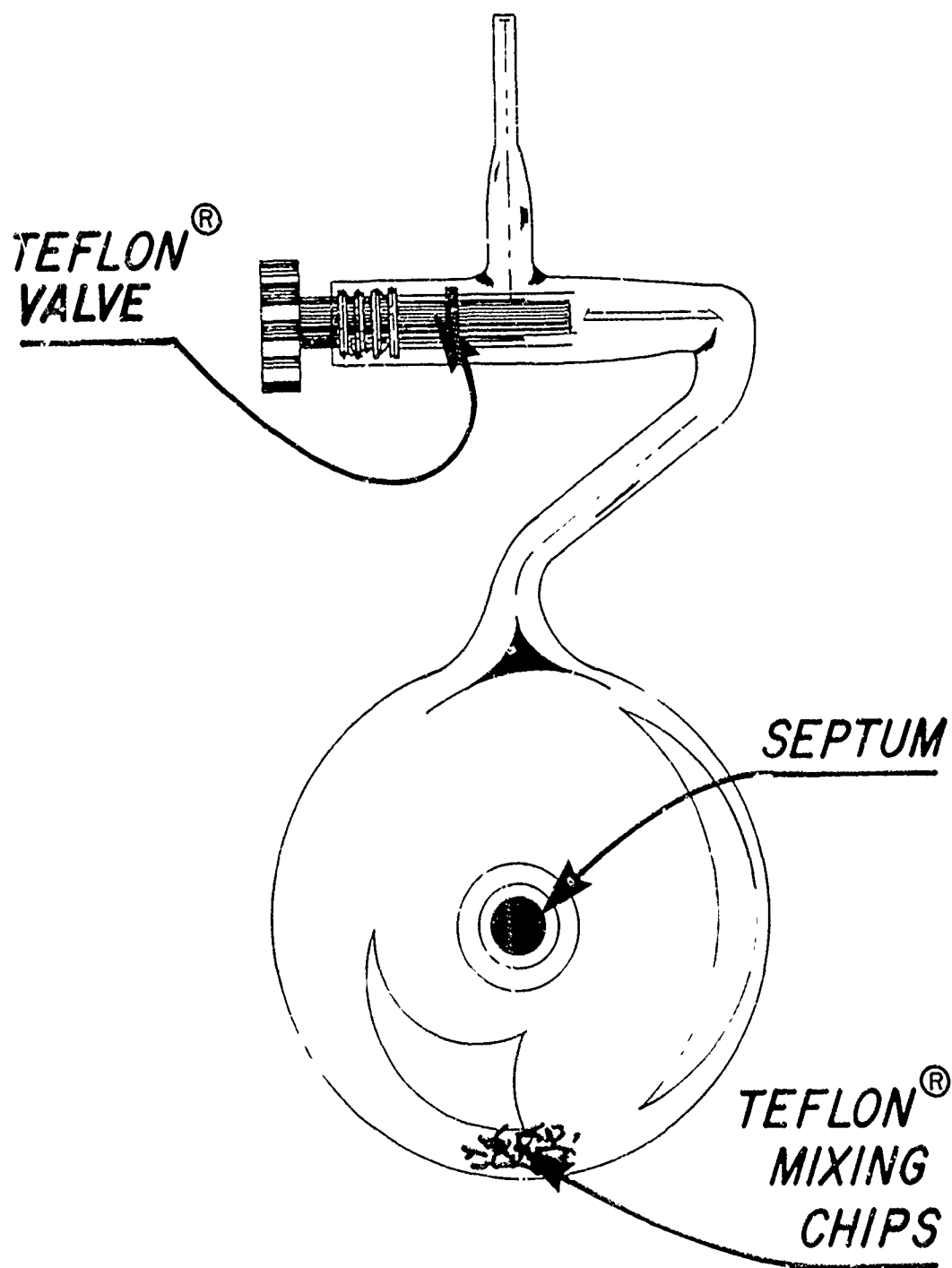


Figure 1. 300-ml Pyrex[®] Reaction Flask

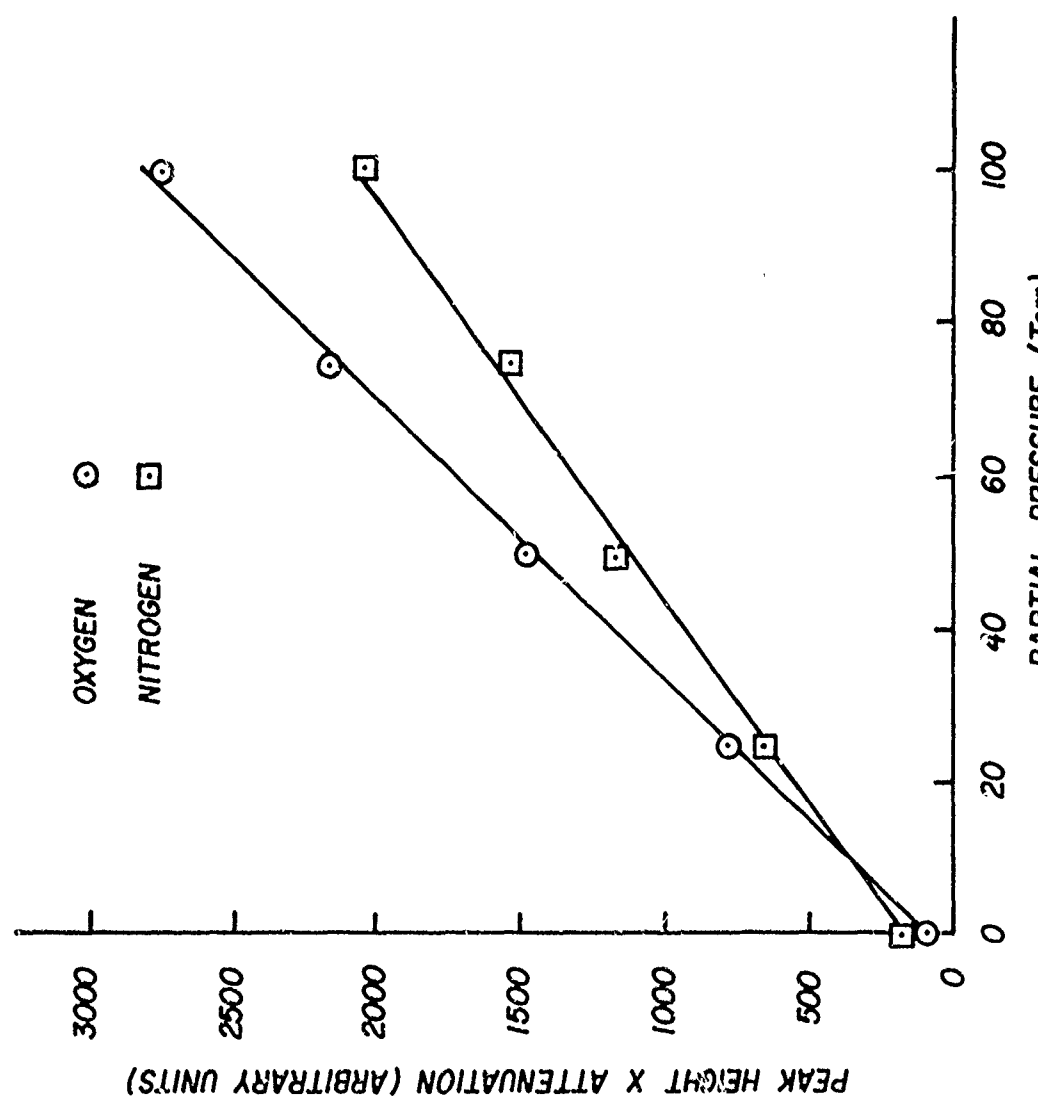


Figure 2. GC Calibration Curve for Oxygen and Nitrogen

Hydrazine concentration was not followed during the experimental runs in the 300-ml flask. Possible ammonia formation was also unconfirmed due to detection constraints.

RESULTS

Two sets of experiments were conducted. One with the plain 300-ml flask and a second where enough Teflon[®] chips were added to approximately double the surface area. Hydrazine vapor pressure was found from the relation (Reference 5)

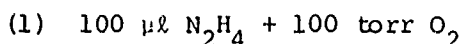
$$\log P \text{ (mm)} = 6.50603 \frac{653.880}{(T, {}^\circ\text{K})} + 0.047914 (T, {}^\circ\text{K}) - 4.9886 \times 10^5 (T, {}^\circ\text{K})^2.$$

At 22 °C this equation gives 11.8 torr. It should be noted that 100 μl of hydrazine corresponds to 3.15×10^{-3} moles, whereas oxygen partial pressures of 50 and 100 torr represent 0.82×10^{-3} and 1.63×10^{-3} moles respectively, thus, hydrazine was in excess.

Results are summarized in Table 1.

TABLE 1. HYDRAZINE OXIDATION RESULTS (300-ML FLASK)

a. Regular Surface Area



Time (min)	P_{O_2} (torr)	P_{N_2} (torr)	$P_{\text{O}_2} + P_{\text{N}_2}$ (torr)
0	103.1	0	103.1
8	68.7	43.4	112.1
12	60.4	45.1	105.5
15	50.9	52.0	102.9
20	43.8	60.6	104.4
25	36.7	67.6	104.3
30	32.0	72.8	104.8
35	26.0	76.2	102.2
40	22.5	77.9	100.4
45	18.9	79.7	98.6
50	15.3	83.1	98.4
55	13.0	84.9	97.9
60	11.8	90.1	101.9
		average	102.8 ± 3.8

(2) $100 \mu\ell N_2H_4 + 50 \text{ torr } O_2$

<u>Time (min)</u>	<u>P_{O_2} (torr)</u>	<u>P_{N_2} (torr)</u>	<u>$P_{O_2} + P_{N_2}$ (torr)</u>
0	54.5	0	54.5
2	49.1	19.1	68.2
10	37.3	29.5	66.8
15	32.6	30.4	63.0
20	29.6	34.7	64.3
25	26.6	38.2	64.8
30	21.8	39.9	61.7
35	18.3	41.6	59.9
40	16.6	45.1	61.7
45	14.8	46.8	61.6
			average <u>62.6</u> \pm 3.8

(3) $1000 \mu\ell N_2H_4 + 100 \text{ torr } O_2$

<u>Time (min)</u>	<u>P_{O_2} (torr)</u>	<u>P_{N_2} (torr)</u>	<u>$P_{O_2} + P_{N_2}$ (torr)</u>
0	98.3	0	98.3
1	92.4	20.9	113.3
5	84.1	20.9	105.0
10	79.4	26.1	105.5
15	74.6	31.2	105.8
20	69.9	33.0	102.9
25	65.1	34.7	99.8
30	62.8	36.4	98.5
35	62.8	39.9	102.7
40	58.0	39.9	97.9
45	56.9	41.6	99.8
			average <u>102.7</u> \pm 4.6

b. High Surface Area (i.e., with added Teflon chips)

(1) $100 \mu\ell N_2H_4 + 100 \text{ torr } O_2$

<u>Time (min)</u>	<u>P_{O_2} (torr)</u>	<u>P_{N_2} (torr)</u>	<u>$P_{O_2} + P_{N_2}$ (torr)</u>
0	114.9	7.0	121.9
2	81.7	49.1	130.8
6	52.7	71.0	123.1
9.5	34.3	81.4	115.7
13	27.2	95.2	122.4
16	21.3	98.7	120.0
20	16.6	103.9	120.5
25	11.8	107.4	119.2
30	8.3	110.8	119.1
			average <u>121.4</u> \pm 4.2

(2) $100 \mu\text{l} \text{N}_2\text{H}_4 + 50 \text{ torr O}_2$

<u>Time (min)</u>	<u>P_{O_2} (torr)</u>	<u>P_{N_2} (torr)</u>	<u>$P_{O_2} + P_{N_2}$ (torr)</u>
0	55.7	0	55.7
1	41.4	19.1	60.5
5	19.5	37.3	56.8
10	7.7	48.5	56.2
15	2.9	53.7	56.6
20	0.6	54.5	55.2
			average 56.8 ± 1.9

(3) $1000 \mu\text{l} \text{N}_2\text{H}_4 + 100 \text{ torr O}_2$

<u>Time (min)</u>	<u>P_{O_2} (torr)</u>	<u>P_{N_2} (torr)</u>	<u>$P_{O_2} + P_{N_2}$ (torr)</u>
0	112.6	0	112.6
1	94.8	20.8	115.6
5	67.5	43.4	110.9
10	42.6	67.6	110.2
15	26.0	83.1	109.1
20	15.4	95.2	110.6
25	8.3	98.7	107.0
30	3.5	103.9	107.4
			average 110.4 ± 2.8

The consistency of the oxygen plus nitrogen partial pressures is good evidence for the simple overall oxidation:



This is in agreement with the findings of Bowen and Birley (Reference 4).

The decay in oxygen partial pressure followed first order kinetics. The results are shown in Table 2. Half lives were calculated as follows:

$$\text{half life} = \log_e 2 / (-m)$$

where m is the slope of the line which gives the best fit to a plot of \log_e (oxygen partial pressure) versus time.

TABLE 2. REACTION KINETIC RESULTS FOR HYDRAZINE OXIDATION
IN THE 300-ML PYREX FLASK

Sample Composition	Regular Surface			Teflon [®] Chips Added		
	Slope	half life(min)	corr coeff	Slope	half life(min)	corr coeff
100 μl N_2H_4 100 torr O_2	-0.036	19.5	0.942	-0.084	8.2	0.989
100 μl N_2H_4 50 torr O_2	-0.029	24.2	0.986	-0.215	3.2	0.995
1000 μl N_2H_4 100 torr O_2	-0.012	60.3	0.956	-0.109	6.3	0.994

These results show that oxidation is fairly rapid, especially in the presence of relatively high surface to volume ratios. The good correlation coefficients lend further support to first order oxygen dependence in the oxidation reaction.

Finally, in runs with no oxygen present in regular and high surface area configurations, only about five torr of nitrogen were produced in reaction times of 45 and 30 minutes respectively. This indicates that non-oxidative hydrazine removal was relatively insignificant on the time scale of these experiments.

SECTION IV
OXIDATION IN A 55-LITER REACTION CELL

EXPERIMENTAL

The availability of a long path infrared cell led to the second study of hydrazine oxidation in air. The cell used in this study consisted of a 10-foot by 6-inch section of Pyrex[®] glass pipe with internal multiple reflection optics of the type described by White (Reference 6). Though capable of path lengths of up to 200 meters, the cell was severely path limited in this study because of detector sensitivity and optical coupling deficiencies. Because of the limitations involved, the experiments discussed in this section were carried out at a path length of about 25 meters. Hydrazine concentration was monitored with a Digilab Model FTS-20 infrared spectrophotometer which had been modified by removing the interferometer from the original optical compartment and replacing the original source with a globar source operated from a Variac transformer in series with a 100-watt incandescent lamp at 96 volts AC. The cell and peripheral equipment are shown schematically in Figure 3.

Materials were introduced into the cell through an external gas manifold or a silicon rubber septum. The cell and manifold were evacuable to less than 20 millitorr Hg with a rotary vacuum pump, as measured with a Hastings Model UH-3 thermocouple gauge. Hydrazine samples were carried into the cell in a stream of nitrogen. Concentrations were in the 500 ppm range. Experiments were carried out by introducing a sample of hydrazine into the cell with nitrogen and bringing the pressure to 504 torr as measured with a Wallace and Tiernan Model 61B-1D-0800 absolute pressure gauge. The sample was allowed to equilibrate overnight, then 126 torr of oxygen were added and the reaction was followed for 6 to 8 hours.

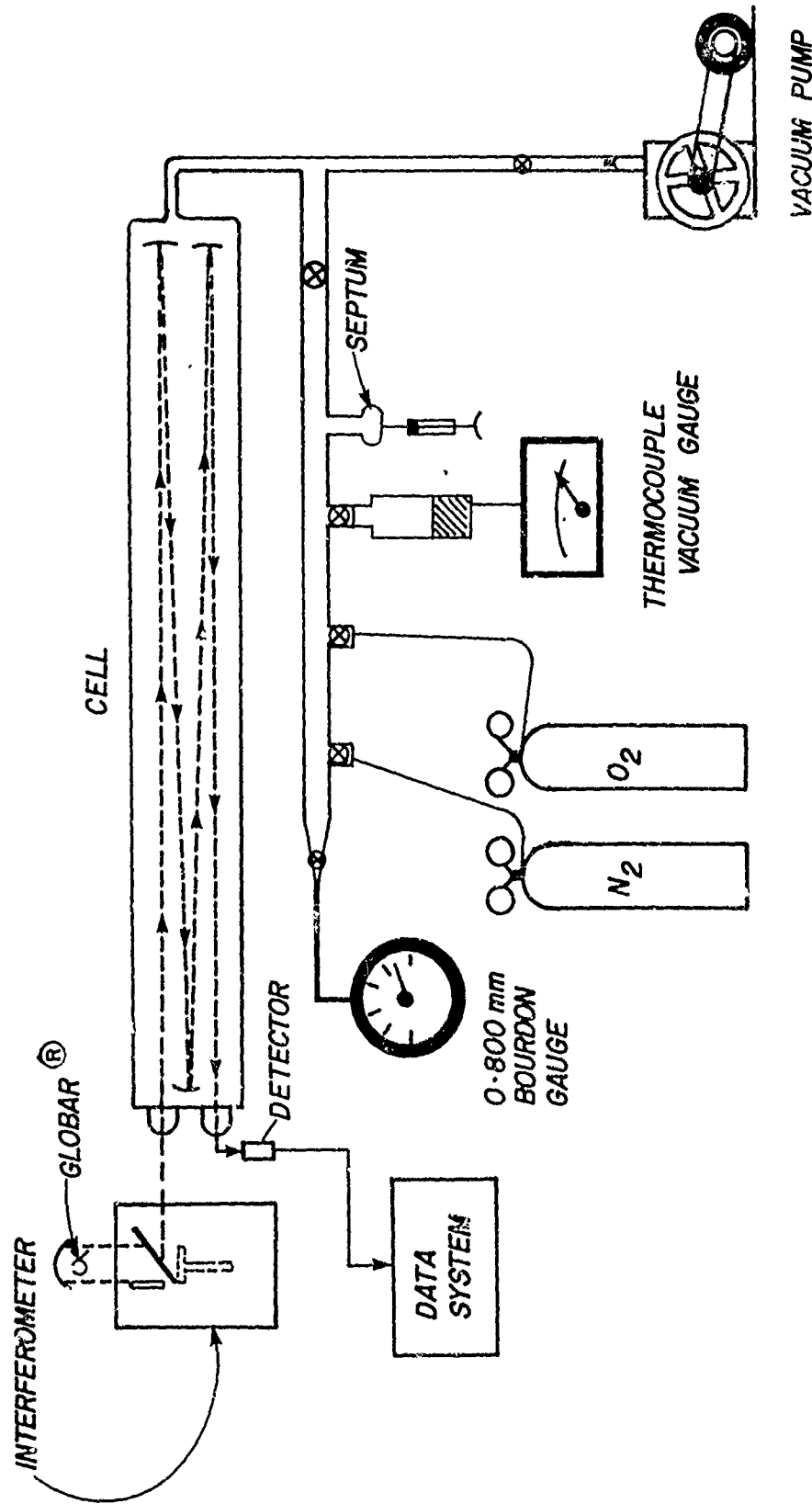


Figure 3. Long Path Reaction Cell and Peripheral Equipment

Hydrazine absorbance was monitored at 4 cm^{-1} resolution in the N-H asymmetric bending region (Reference 7) at 1606 cm^{-1} . Absorbance calibration curves were generated for hydrazine (Figure 4) and water. The water curve was necessary in order to correct for water absorbance at 1606 cm^{-1} . In order to be able to measure the water absorbance accurately with hydrazine present, its calibration curve was generated by measuring the absorbance at 1869 cm^{-1} and at 1606 cm^{-1} then finding the ratio of the two absorbances. In this way, water absorbance could be measured at 1869 cm^{-1} without hydrazine interference then related to water absorbance at 1606 cm^{-1} and corrected for. In a series of 15 runs with only water vapor and air in the cell, absorbances were measured at 1869 cm^{-1} and 1606 cm^{-1} . The relationship which gave the best fit was:

$$A_{1606\text{ cm}^{-1}} = 0.061 + 0.223 A_{1869\text{ cm}^{-1}} + 0.003 (A_{1869\text{ cm}^{-1}})^2.$$

This equation was written into a FOCAL program which would accept as input the measured absorbance at 1869 cm^{-1} and 1606 cm^{-1} and give as output the hydrazine and water concentrations in ppm. The output was stored in separate, retrievable data files. The program was run on a Digital Equipment Corporation pdp 8/m minicomputer. Listings of the absorbance calculation program and the program which lists the data files are given in the Appendix.

Baseline values for hydrazine disappearance and water formation were established by making runs where only nitrogen and hydrazine were added to the cell. After these runs, about 20 oxidation experiments were conducted.

RESULTS

The results of these experiments, while similar, show considerable scatter. Two representative runs are used to show the spread of data

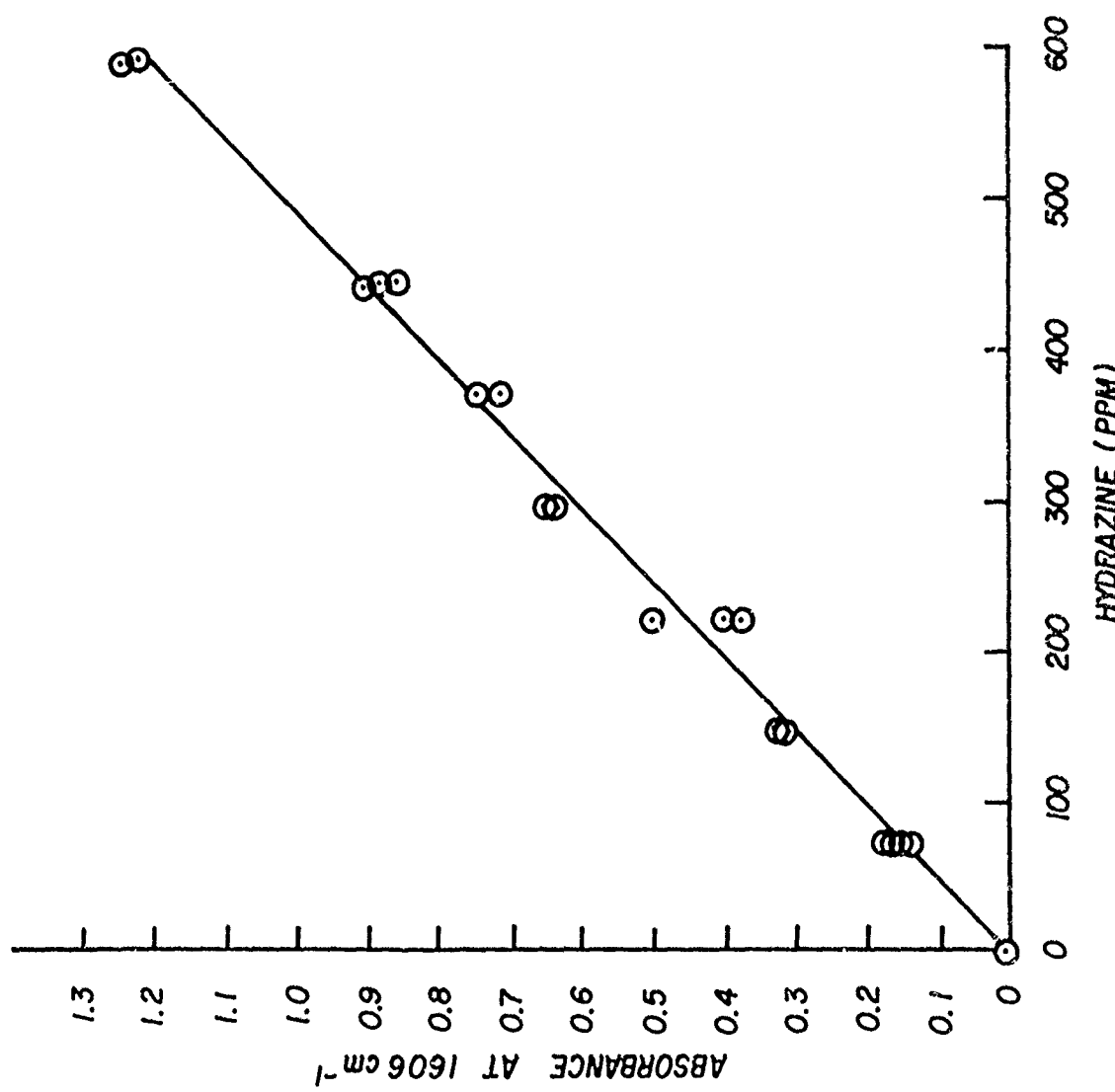


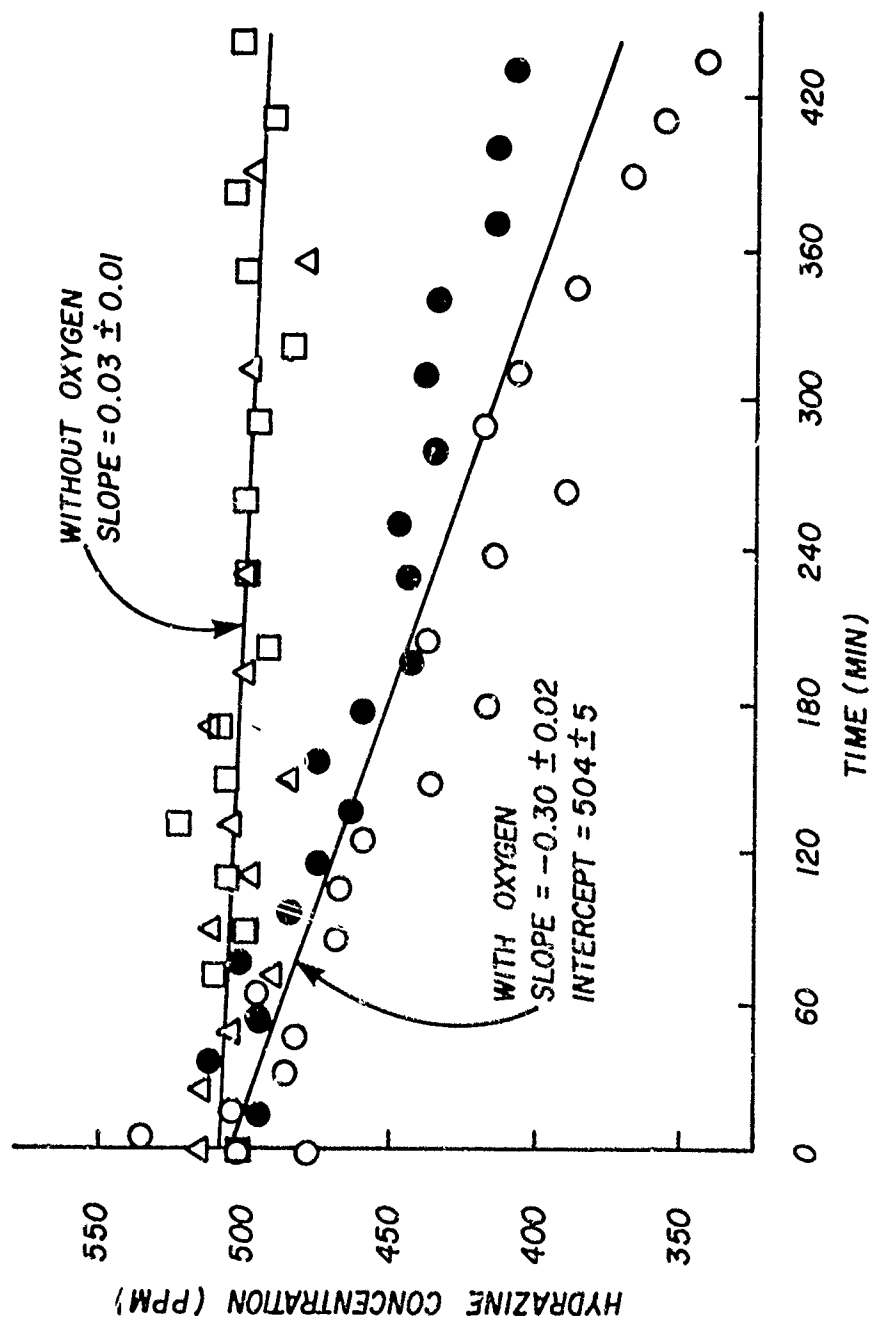
Figure 4. Hydrazine Calibration Curve (Long Path Cell)

points in hydrazine decay and water production both with and without oxygen. The results are shown in Figures 5 and 6, where hydrazine concentrations are normalized to a starting value of 500 ppm and water concentrations to 0 ppm.

From Figures 5 and 6 it is evident that about 100 ppm hydrazine react in 400 minutes and about 100 ppm water are formed in 400 minutes. This is consistent with the products of the proposed reaction $N_2H_4 + O_2 \rightarrow 2H_2O + N_2$ but not the stoichiometry. This lack of water is not completely understood but is probably explained, at least in part, by adsorption or condensation processes within the chamber.

By assuming pseudo first order decay of the hydrazine, and using the data points of Figure 5, the half-life of hydrazine under these experimental conditions may be estimated from $\ln(2)/m$, where m is the slope of the plot of \ln hydrazine concentration versus time. A least squares calculation process gives a half-life of 16 ± 3 hours with a correlation coefficient of 0.90.

During the course of these experiments some runs were made at lower initial hydrazine concentrations. This made the appearance of the ammonia inversion doubled symmetric bending bands (Reference 8) at 932 and 968 cm^{-1} clearly visible during the later stages of the reaction. This was the first evidence in these experiments that ammonia was also being produced, however, no attempt was made to quantitate its production during this phase of experimentation.



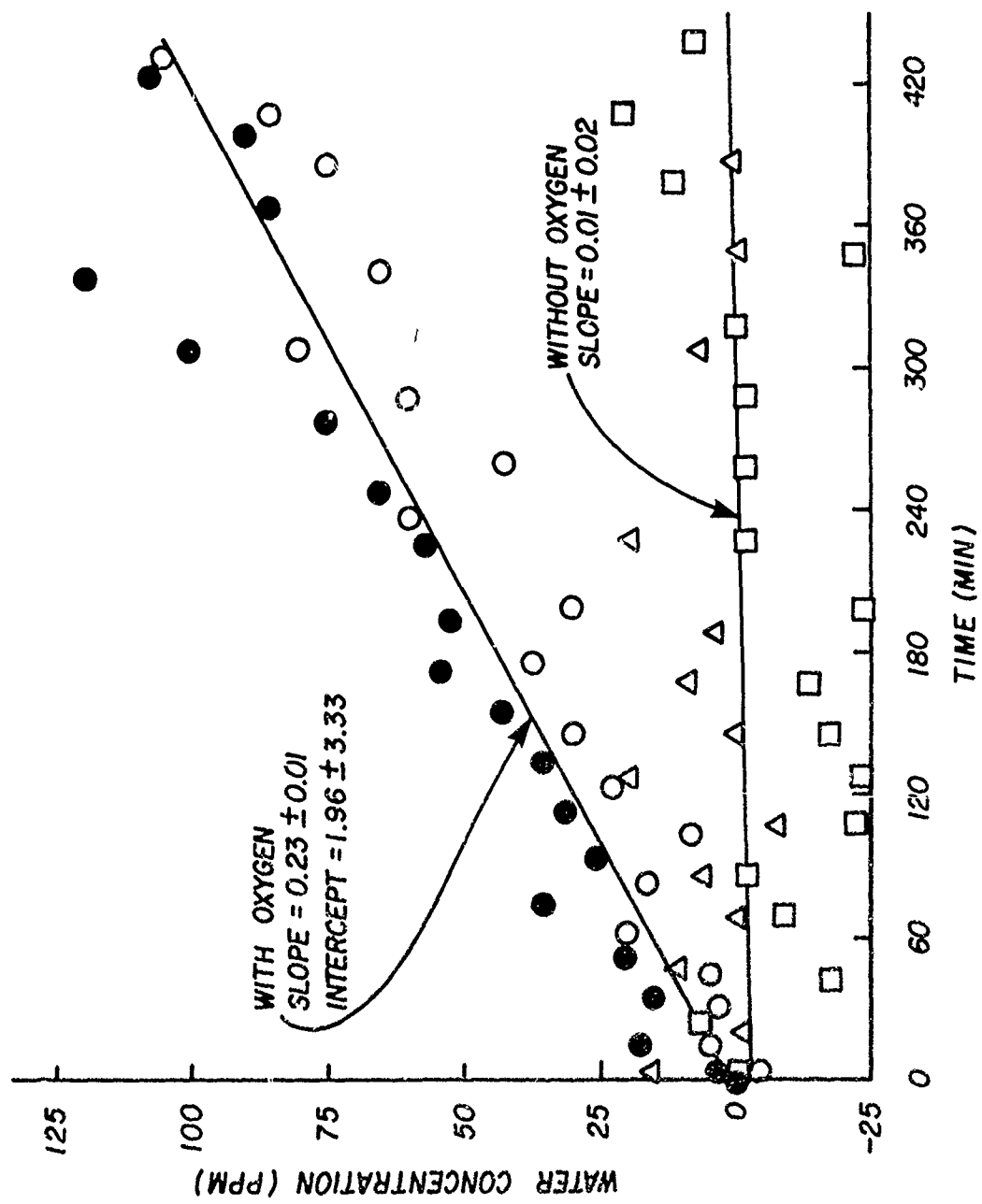


Figure 6. Plot of Water Concentration versus Time for the 55-Liter Cell
(Note: each different symbol represent a separate experimental run)

SECTION V
OXIDATION IN REACTION VESSELS OF DIFFERENT SURFACE TO VOLUME RATIOS

EXPERIMENTAL

During this phase of the study, several different reaction vessels were employed to study the effect of surface to volume ratio on the rate of hydrazine oxidation. In the early experimental stages, the reaction vessel consisted of a Pyrex® carboy with a vacuum manifold attached. Hydrazine was injected as a liquid through a septum and carried into the carboy with the fill gas. Reaction progress was followed by attaching a 10-cm infrared gas cell to the vacuum manifold, evacuating the cell and manifold, then admitting a sample from the carboy at its prevailing pressure. An infrared spectrum of the sample was then obtained. There were several problems associated with this system mainly involving reactant input and valid sampling during the reaction.

To overcome these problems, another system was constructed with the carboy attached to the vacuum manifold as before, but where the reaction mixture was continuously pumped through a 10-cm infrared flow-through cell. Hydrazine was vaporized into the system and a synthetic air atmosphere was metered into the carboy. The spectrometer recorded spectra every 30 seconds while continuous pumping from the middle of the carboy was maintained by a Teflon® coated diaphragm pump through 1/8-inch Teflon® tubing. Due to the materials used in this system it was felt that inertness could be maintained while overcoming mixing and sampling problems. Later work showed, however, that the reaction in this system was almost totally dominated by surface catalyzed, heterogeneous effects.

The system which finally seemed to overcome all of the earlier problems consisted of a reaction vessel with demountable, o-ring sealed windows, and an outlet to the vacuum manifold. This vessel (Figure 7) was mounted external to the spectrometer and the infrared

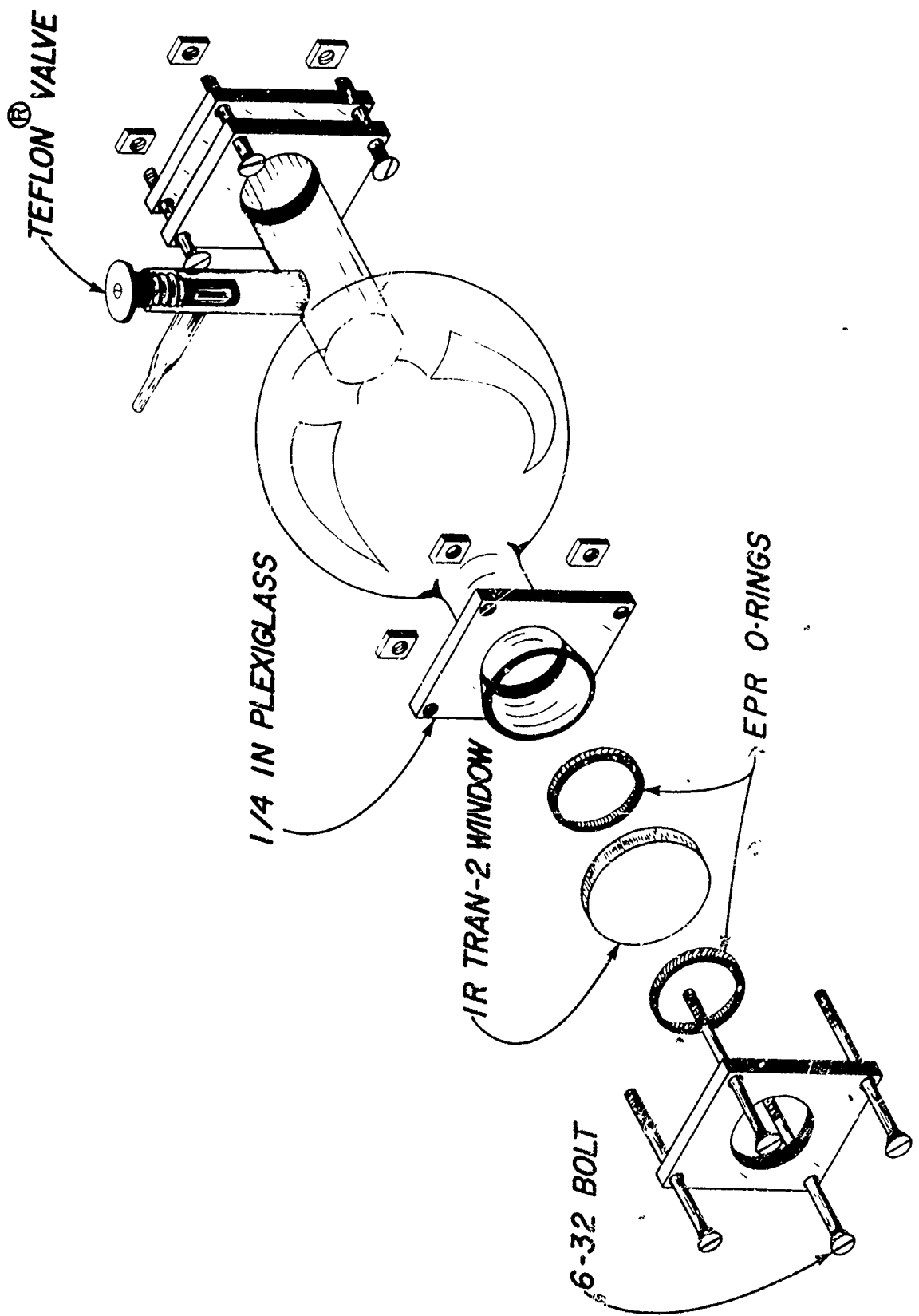


Figure 7. 5-Liter Pyrex[®] Reaction Vessel (Showing Exploded View of Window Mounting System)

beam was passed from an external Globar[®] source, through the reaction vessel and into the spectrometer. The Globar[®] was operated in series with a 100-watt light bulb directly from a variable transformer at 96 volts AC. The entire optical system and vacuum manifold are shown in Figure 8.

Experimental runs were conducted in the following manner. The entire system, including the 5-liter flask was pumped down to <10 millitorr. Then hydrazine was expanded into the system to a pressure of about 5 torr. Finally, the pressure was brought to 605 torr with nitrogen. At this point, the sample was allowed to equilibrate for 30 minutes. At this time, a spectrum was recorded (60 coadded scans, resolution 4 cm^{-1}), and another spectrum was recorded 15 minutes later. These two spectra were used to establish the initial absorbance value and stability of the sample. Then oxygen was added to bring the total pressure to 760 torr and additional spectra were recorded every 30 minutes for 5 or 6 hours.

To facilitate generation of calibration curves, as well as have a high surface area to volume cell, an additional vessel was constructed (herein after referred to as the 44 x 2 cm cell) to have the same path length and use the same demountable window system (see Figure 7) as the 5-liter flask. Calibration curves for water and ammonia were generated by using this cell, while the hydrazine calibration was done using the 5-liter flask. Known pressures were expanded into the cell or flask as measured with a Texas Instruments Model 145 precision pressure gauge, then the pressure was brought to 760 torr with nitrogen. These calibration curves are shown in Figures 9 and 10. For hydrazine the analytical band used was in the asymmetric NH_2 wagging region (Reference 7) at 910 cm^{-1} ; while for ammonia one of the inversion doubled symmetric NH bending bands (Reference 8) at 968 cm^{-1} was used. The hydrazine calibration curve departs badly from the Beer-Lambert law and was fit suitably only when a third order polynomial was used. A second calibration curve generated at the end of the

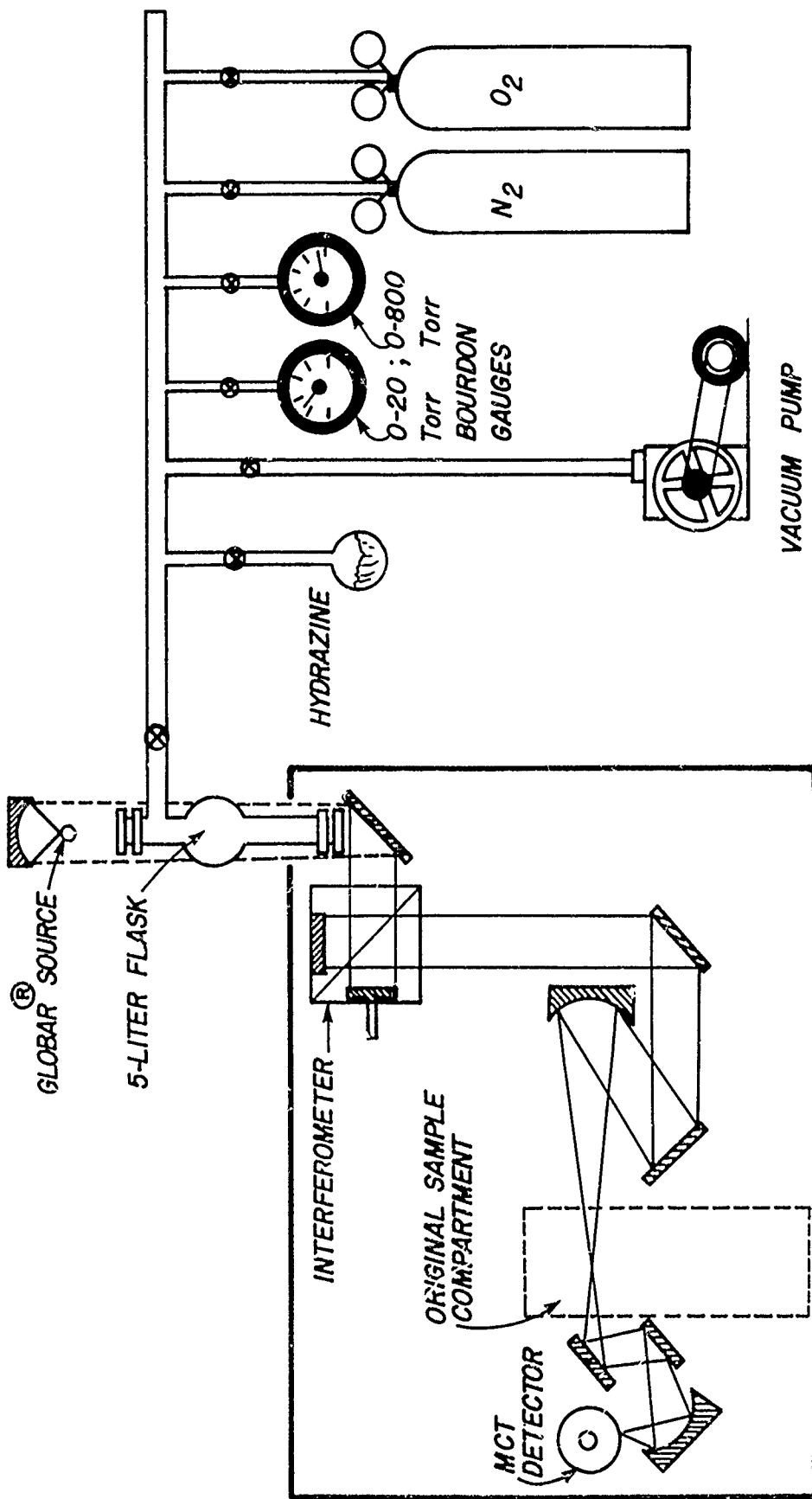


Figure 8. Optical Path and Vacuum Manifold System used with the 5-Liter Flask and 44 x 2 cm Cell

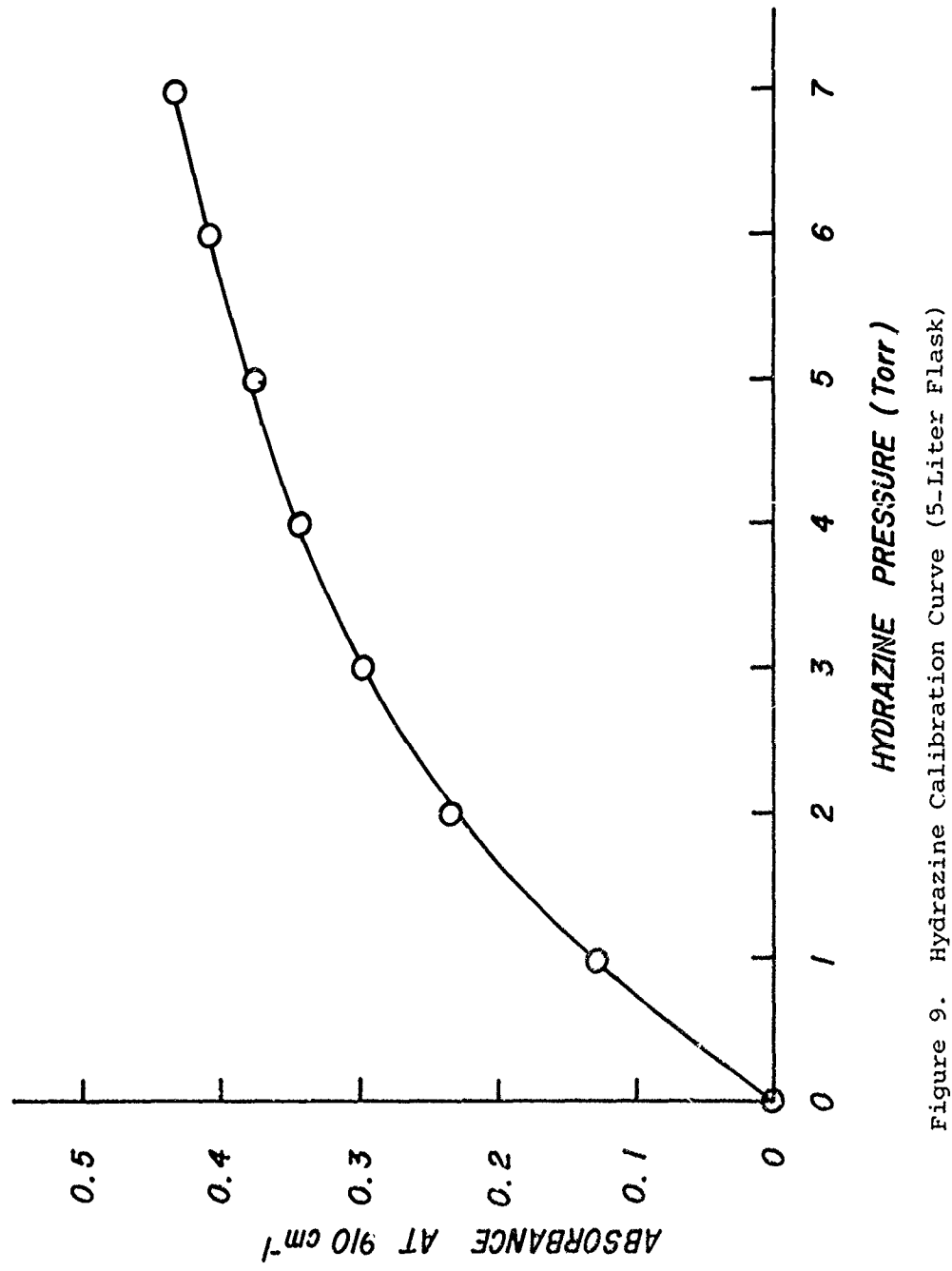


Figure 9. Hydrazine Calibration Curve (5-Liter Flask)

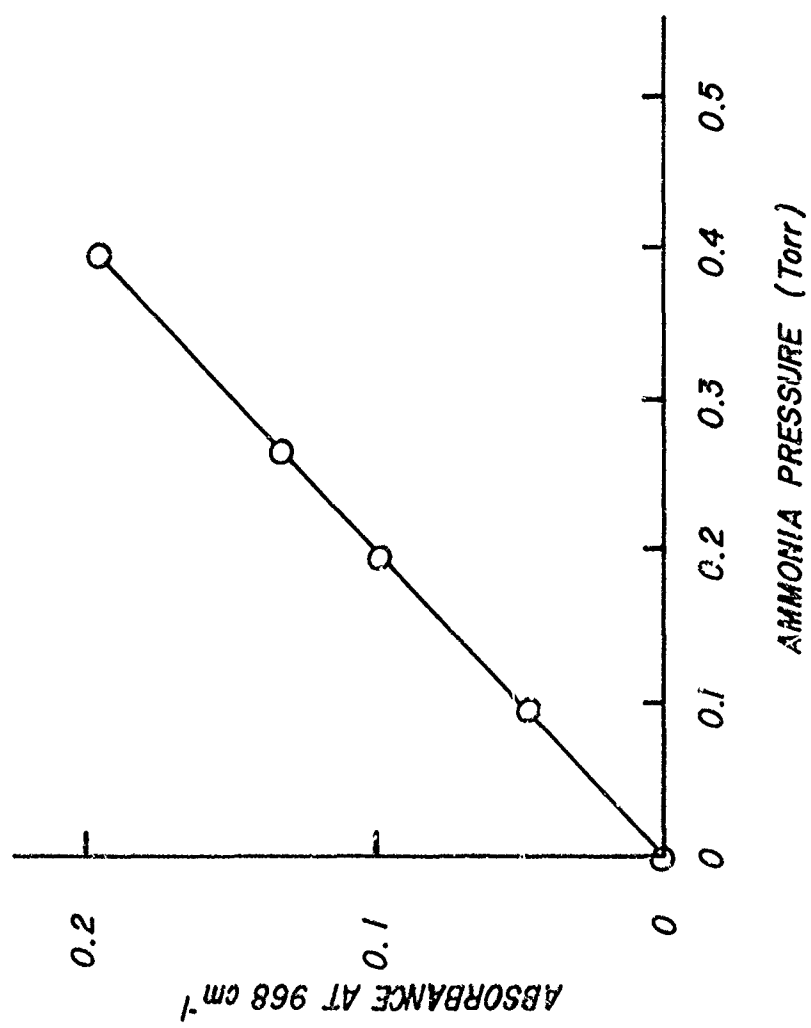


Figure 10. Ammonia Calibration Curve (44 x 2 cm Cell)

experiments reported herein gave experimental hydrazine decay data (in percent of starting material) which were essentially the same as that given by the original calibration curve for any given experimental run. However, absolute values for hydrazine partial pressure for a given absorbance value differed by 5 to 25 percent between the two curves. The decay data remains valid, but absolute pressure values cannot be accurately determined from current absorbance data.

Quantitation of water vapor was not attempted due to lack of control over room humidity and severe departure of the absorbance from linearity in the 1 to 10 torr region. In order to see the relative positions of the absorbance bands of hydrazine, ammonia and water these bands are plotted in Figure 11.

RESULTS

Early oxidation experiments began with the 5-liter flask, and showed a hydrazine oxidation half life of about 25 minutes (see Figure 12). This represented an order of magnitude increase over the system with the diaphragm pump and flow through cell and was very encouraging. However, when the 44 x 2 cm cell was used, the oxidation half life was about 2.5 hours (see Figure 13). This result was confusing since the surface to volume ratio had increased from 0.3 cm^{-1} to 2 cm^{-1} in going from the 5-liter flask to the 44 x 2 cm cell. Further examination of the decay curves for each vessel showed that the surface area was the rate controlling factor (instead of the expected surface to volume ratio) in these particular glass vessels, with the half life being almost directly proportional to the surface area (approximately 1600 cm^2 for the 5-liter flask, and 300 cm^2 for the 44 x 2 cm cell).

To evaluate the effects of reaction vessel surface composition on the rate of the reaction, both vessels were coated with paraffin wax. In the 5-liter flask, the rate decreased dramatically (see Figure 14). This was the expectation since paraffin is often used to coat a reaction

CONDITIONS

RESOLUTION = 4 CM^{-1}
PATH LENGTH = 44 CM
PRESSURE : HYDRAZINE \approx 5 TORR
AMMONIA = .27 TORR
WATER \approx 2 TORR

PLUS
NITROGEN
TO 760
TORR

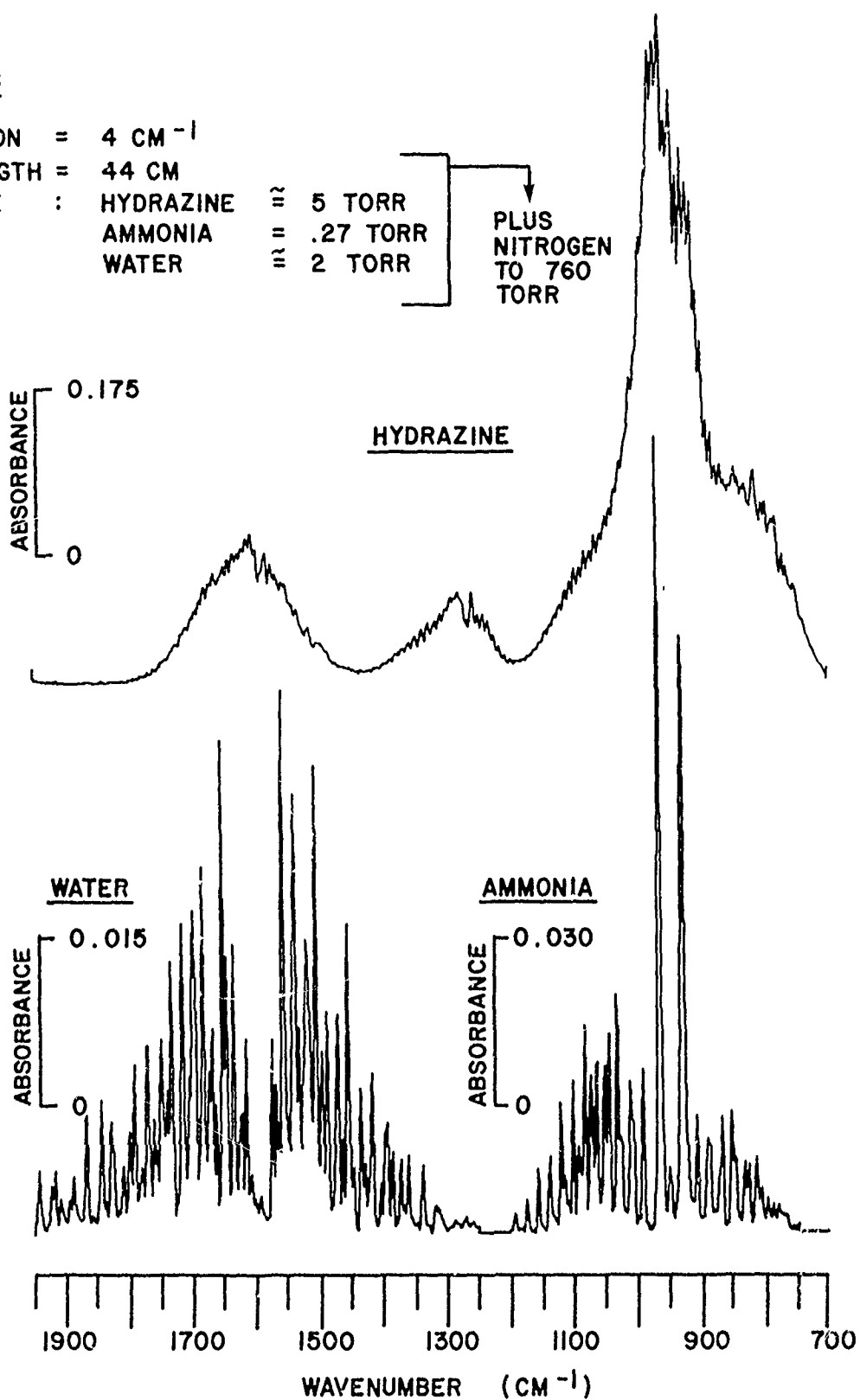


Figure 11. Absorption Spectra of Hydrazine, Water, and Ammonia
Showing Comparative Band Positions

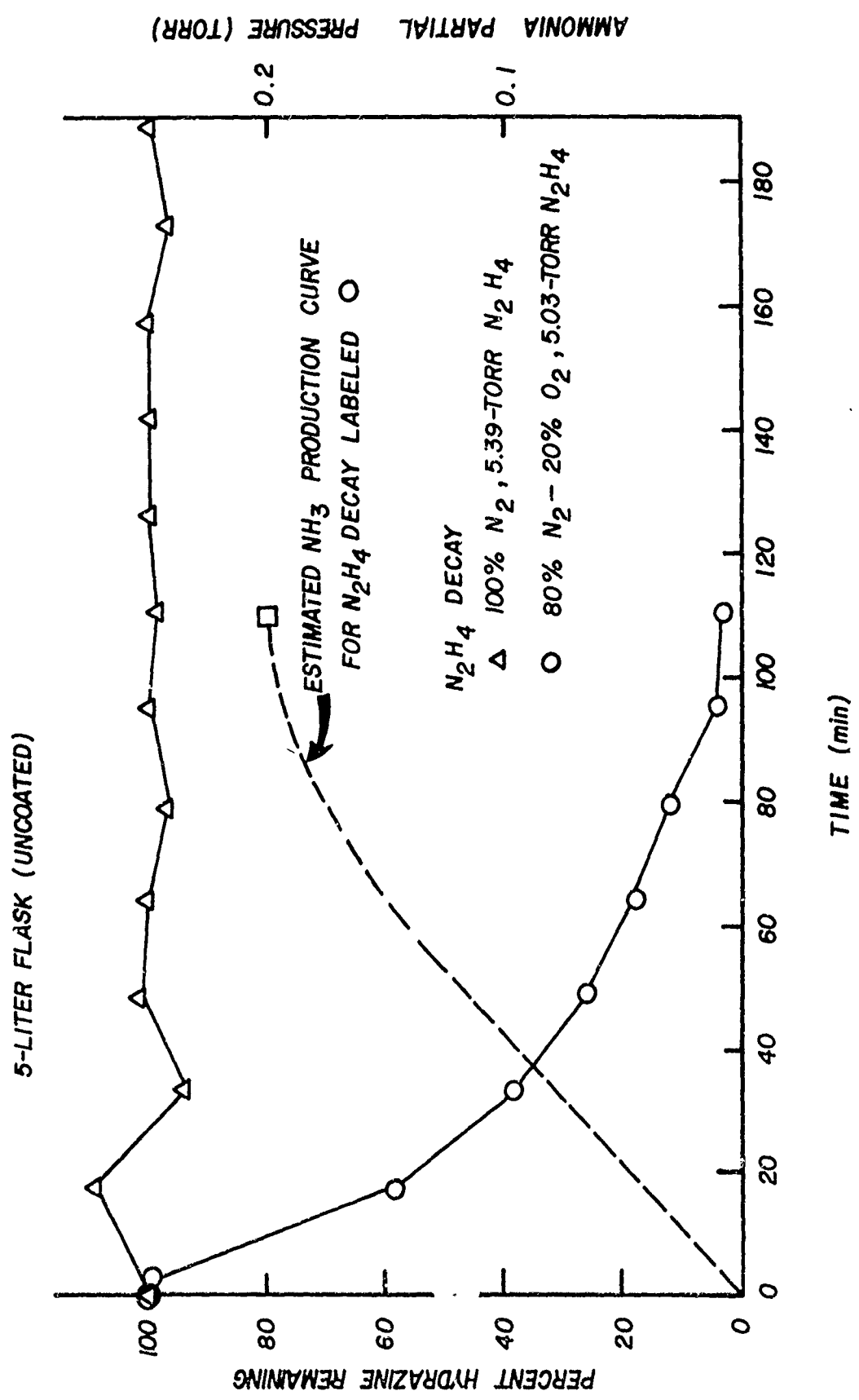


Figure 12. Plots of Hydrazine and Ammonia Concentration Versus Time for the 5-Liter Flask (Uncoated)

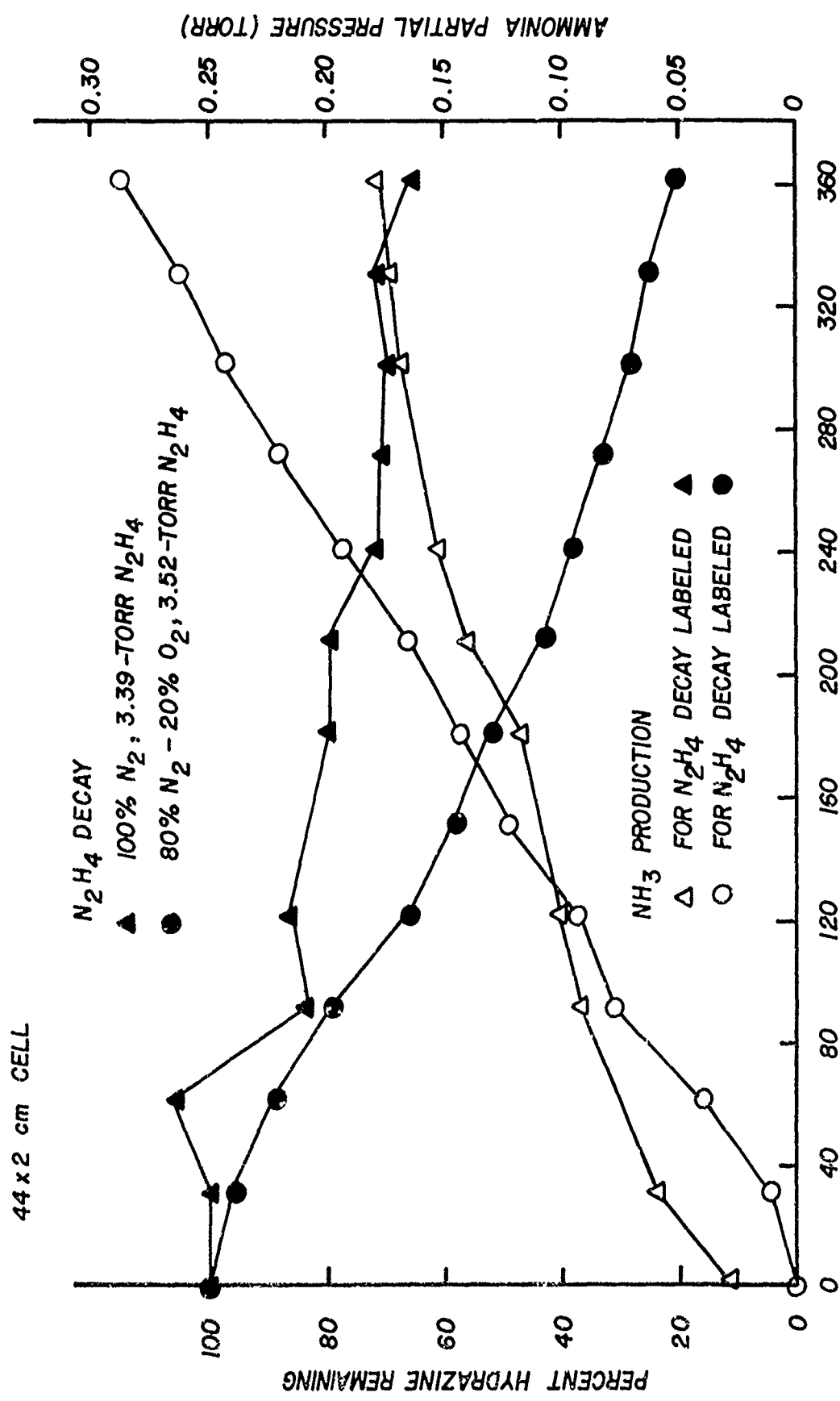


Figure 13. Plots of Hydrazine and Ammonia Concentration versus Time for the 44 x 2 cm Cell

5-LITER FLASK (PARAFFIN COATED)

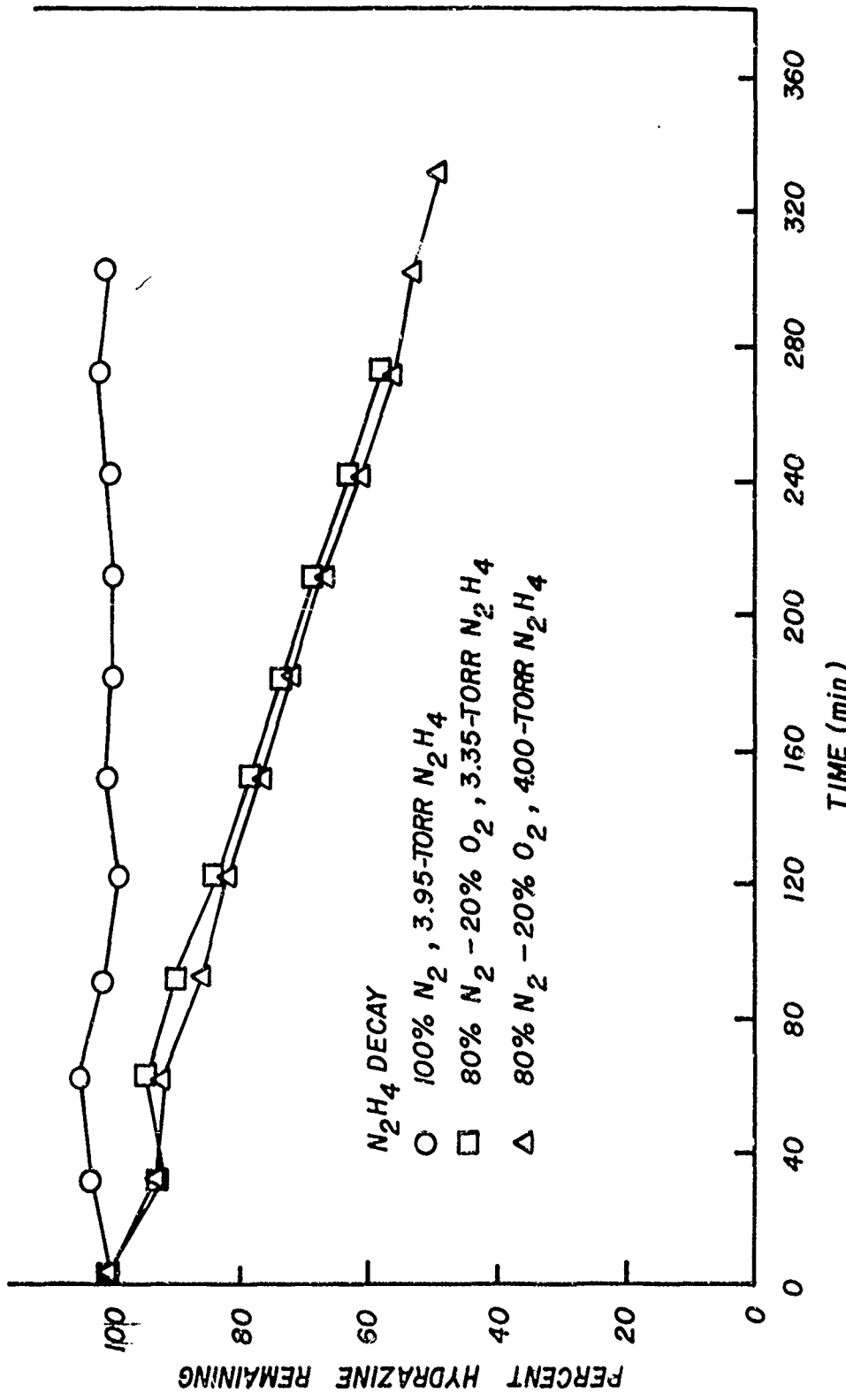


Figure 14. Plots of Hydrazine Concentration versus Time for the 5-Liter Flask
(Paraffin Coated)

vessel and thereby enable its surface activity to be evaluated. When the reaction was run in the paraffin coated 44 x 2 cm cell however, the rate was, if anything, increased slightly. This was a completely unexpected result and seems to indicate, along with evidence on the role of surface area, that there exists a rather complex interplay between surface area, surface composition and surface to volume ratio in the rate controlling step(s) of hydrazine oxidation, at least under the conditions of the current study.

In further experiments (see Figures 15-17) glass tubing (uncoated) or Teflon tubing was added to the reaction vessels to examine the effect of additional surface area and an increase in surface to volume ratio on the reaction rate. In these three cases the effect was similar: the rate was increased approximately in proportion to the increase in either parameter. Thus, it is difficult to say whether the increase in surface area, or surface to volume ratio, or some combination of them was responsible for the observed increased in rate.

It would be desirable to extend this study to actual atmospheric conditions. However, even with the 5-liter flask, the surface to volume ratio is only 0.3 cm^{-1} , whereas a typical ambient value (Reference 9) is $9 \times 10^{-6} \text{ cm}^{-1}$.

Typical spectra recorded at three progressive reaction times are shown for the hydrazine oxidation reaction in Figures 18 and 19. It is clearly evident that ammonia forms during the reaction along with the water. The rate of ammonia production, and thus the total amount produced, is a function of the S/V ratio (see Figures 12, 13 and 17). This enhanced rate of ammonia formation is visible in the spectra recorded with the 44 x 2 cm cell (Figure 19) when compared with spectra recorded at similar times in the 5-liter flask (Figure 18).

Water formation was estimated to exceed hydrazine decay by 25 to 50 percent from a rough calibration curve for water, and by direct comparison of water spectra and oxidation product spectra.

5-LITER FLASK (PARAFFIN COATED, WITH 900 cm OF 0.4 cm PYREX[®] ROD)

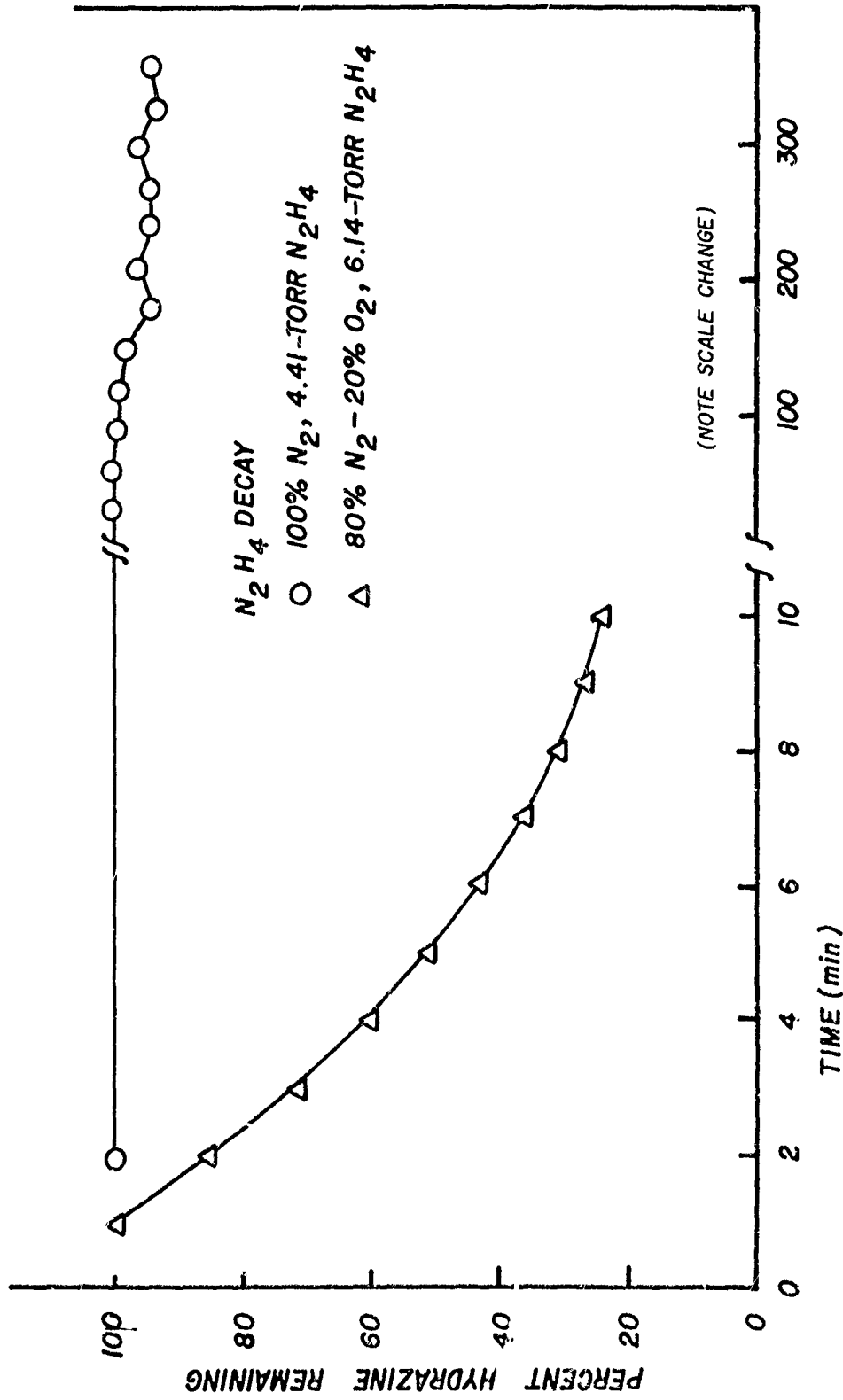


Figure 15. Plots of Hydrazine Concentration versus Time for the 5-Liter Flask (Paraffin Coated with Glass Tubing)

44 x 2 cm CELL (WITH 200 cm OF 1/8 INCH TEFLON[®] TUBING)

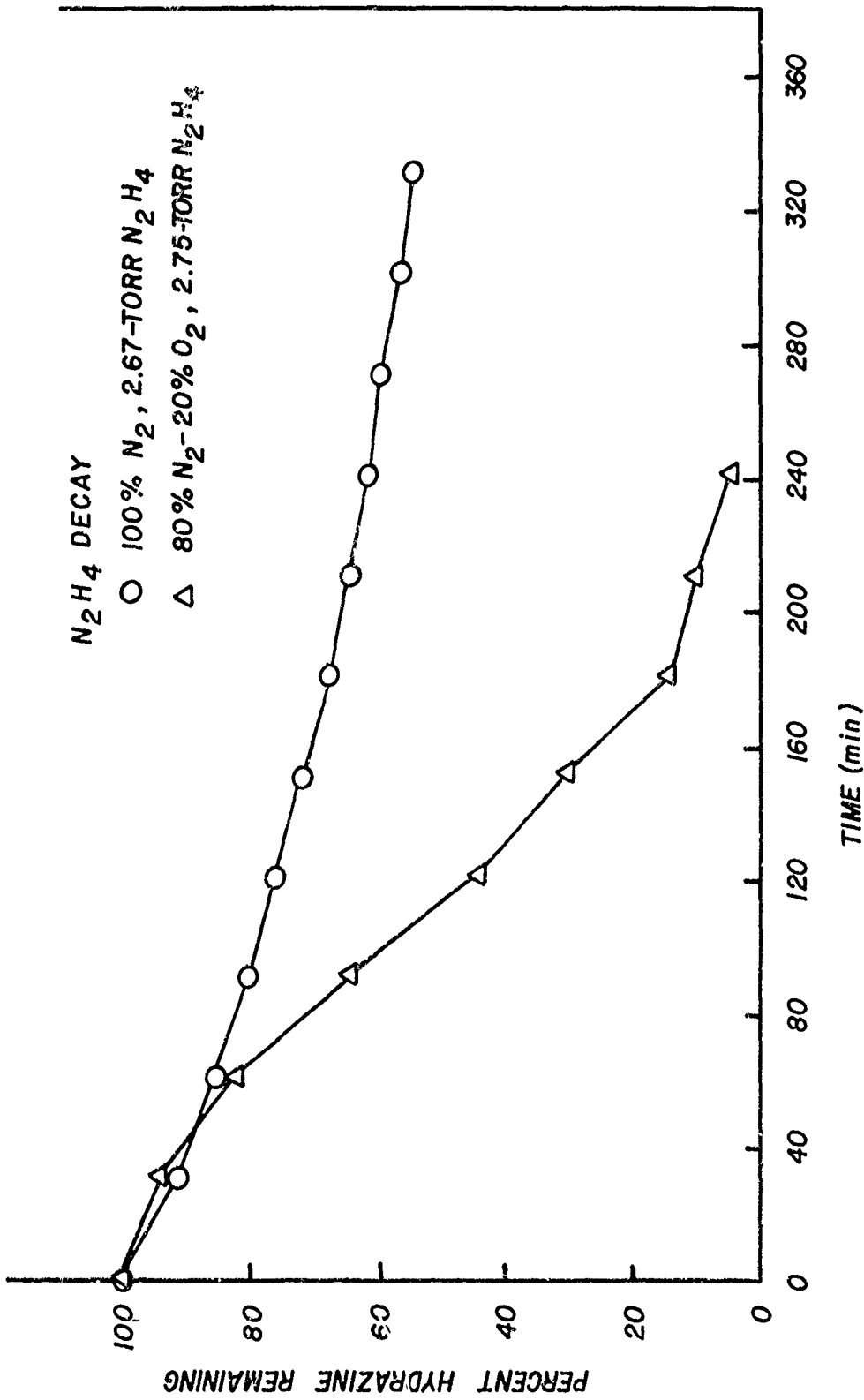


Figure 16. Plots of Hydrazine Concentration versus Time for the 44 x 2 cm Cell (with Teflon[®] Tubing)

44 x 2 cm CELL (WITH 200 cm OF 1/8 INCH GLASS TUBING)

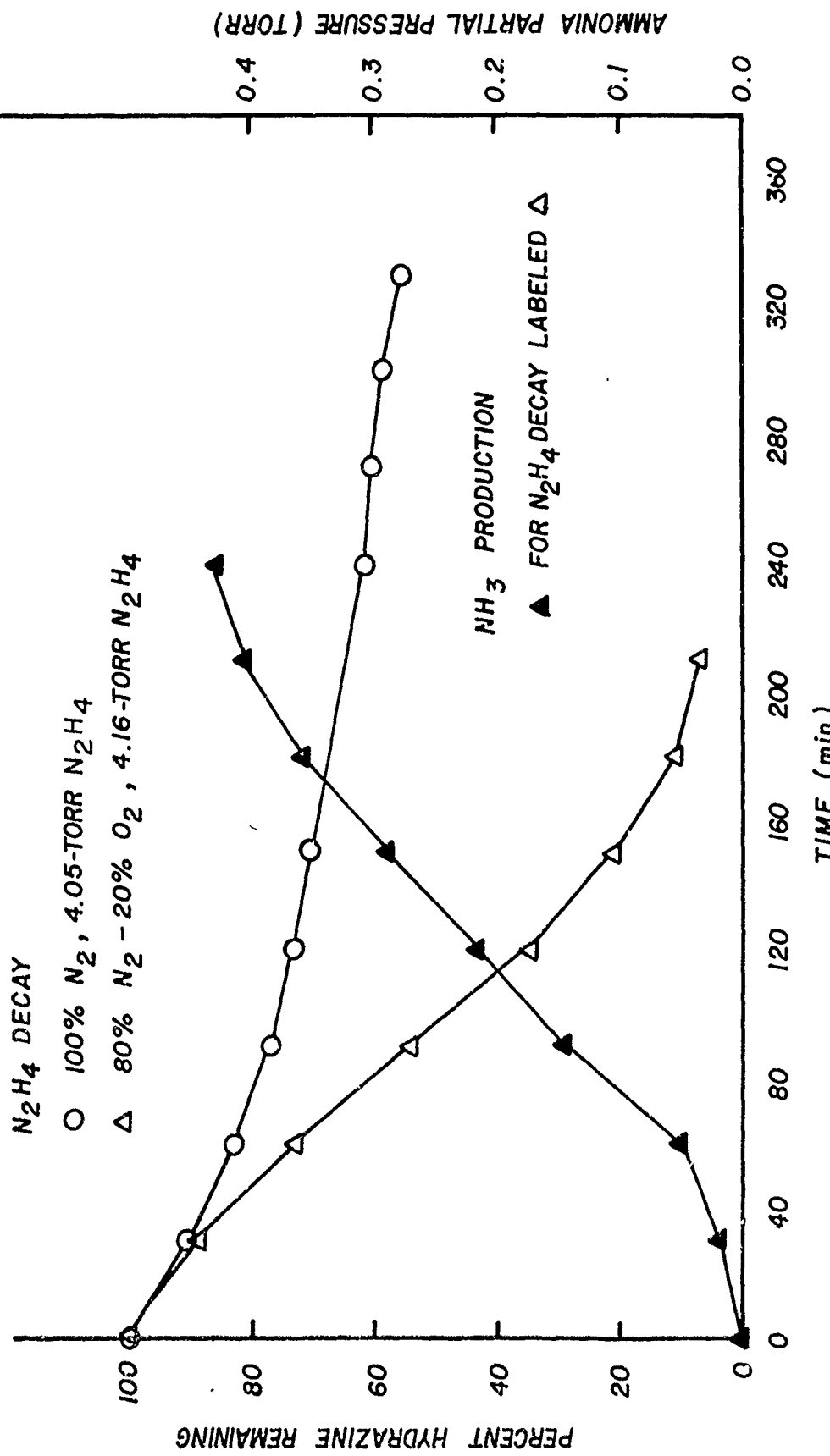


Figure 17. Plots of Hydrazine Concentration versus time for the 44 x 2 cm Cell (with Glass Tubing)

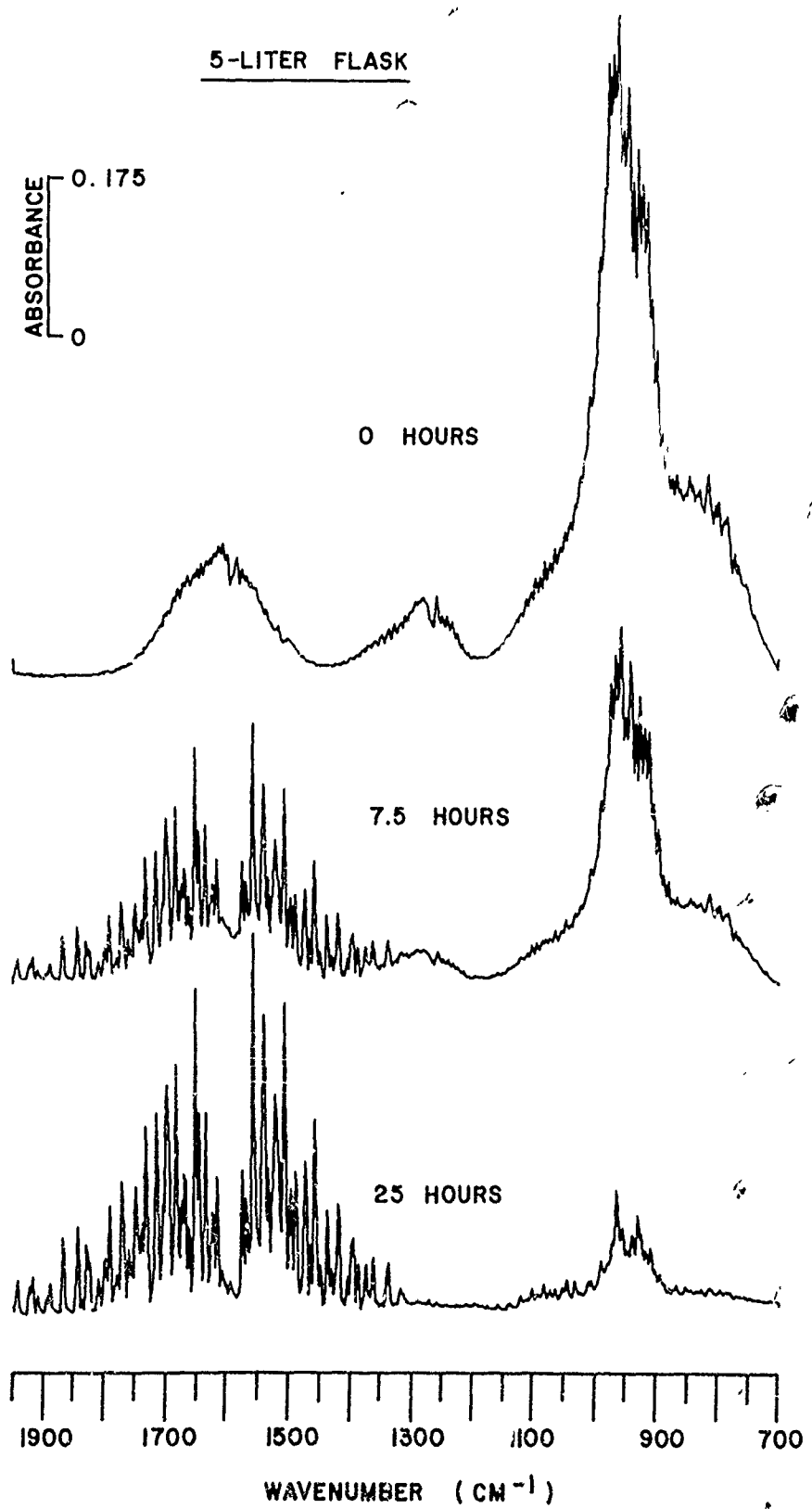


Figure 18. Hydrazine Oxidation Spectra Recorded in the 5-Liter Flask

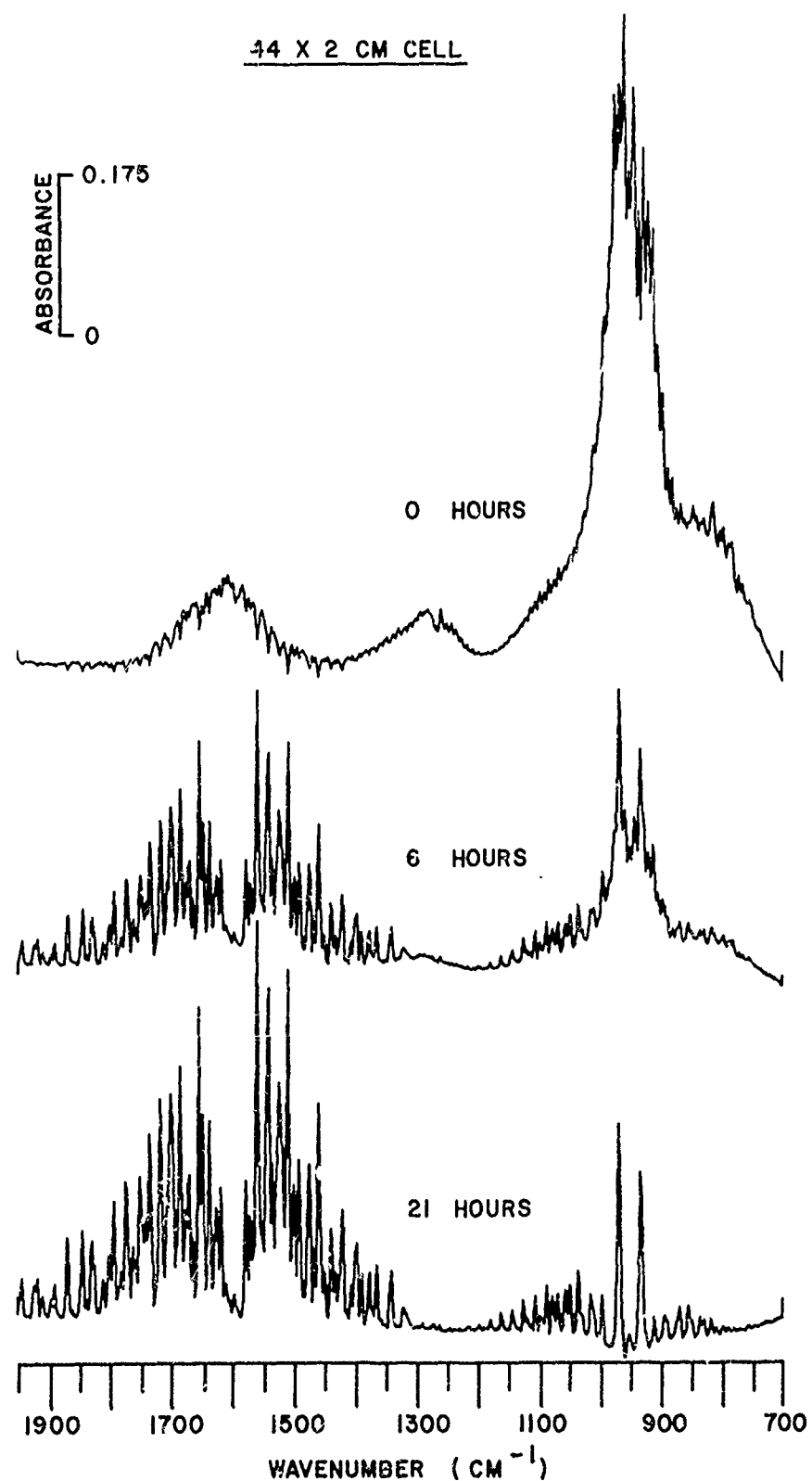


Figure 19. Hydrazine Oxidation Spectra Recorded in the
44 x 2 cm Cell

SECTION VI
CONCLUSIONS

Hydrazine oxidation in air proceeds at a rate strongly dependent upon reaction cell geometry and surface composition. The variation in rate with changes in these parameters is not straight forward. An apparent competition exists among the effects of surface area, surface composition, and surface to volume ratio making it difficult to say which effect is dominant or whether there is some synergism (positive or negative) among them.

In any event, the main reaction under the conditions used in this study is:



It is also clear that there are side reactions which produce ammonia, and that these reactions seem to be mostly heterogeneous.

This study demonstrates that for an accidental hydrazine spill in an enclosed area, decay by oxidation can take up to several hours depending upon variables present at the spill location.

Several areas of additional work are suggested by the results of the present study. An effort to perform real time monitoring of hydrazine concentration in an actual work area under controlled conditions after an intentional spill would be extremely valuable. Further laboratory work designed to elucidate the room temperature mechanisms operating in the hydrazine plus oxygen system is essential. In this regard, there is a need to determine if radicals are involved in the reaction, and, if so, what are the rate controlling steps and the energies associated with them.

The homogeneous reactions of hydrazine in air at the sub part-per-million level need to be explored under very low surface to volume conditions. The chemistry of low levels of hydrazine vapor in polluted urban air needs to be investigated and the activity of different surfaces and materials with respect to heterogeneous decomposition of hydrazine needs to be determined.

REFERENCES

1. Audrieth, L. F. and Ogg, B., The Chemistry of Hydrazine, John Wiley and Sons, Inc., New York, New York, 1951, and references therein.
2. Branch M. C. and Sawyer, R. F., "Review and Evaluation of Rate Data for Gas Phase Reactions of the N-H System", AFOSR-TR-72-0200, Report No. TS-71-1, June 1971, and references therein.
3. Sawyer, C. F., "The Heterogeneous Decomposition of Hydrazine. Part 6. Kinetics of the Decomposition on Supported Palladium and Platinum Catalysts", RPE Technical Report No. 31, November 1974. (and related references).
4. Bowen, E. J. and Birley, A. W., "The Vapor Phase Reaction between Hydrazine and Oxygen", Transactions of the Faraday Society, 47, 580 (1951).
5. Marsh, W. B. and Knox, B. K., USAF Propellant Handbooks Hydrazine Fuels, Vol. 1, AFRPL-TR-69-149, Mar 1970.
6. White, J. L., "Long Optical Paths at Large Aperture", Journal of the Optical Society of America, 32, 285 (1942).
7. Giguere, P. A. and Liu, I. D., "On the Infrared Spectrum of Hydrazine", Journal of Chemical Physics, 51, 4457 (1969).
8. Herzberg, G. W., Molecular Spectra and Molecular Structure II. Infrared and Raman Spectra of Polyatomic Molecules, Van Nostrand Reinhold Co., New York, 1945.
9. The National Research Council, Ozone and other Photochemical Oxidants, National Academy of Sciences, Washington DC, 1977, p. 66.

THIS PAGE IS BEST QUALITY PRACTICABLE
FROM COPY FURNISHED TO DDC

APPENDIX

COMPUTER PROGRAMS FOR HYDRAZINE DATA PROCESSING AND STORAGE

C-PS/8 FOCAL, 1971

```
01.10 C HYDRAZ--ATMOSPHERIC OXIDATION OF HYDRAZINE, DATA REDUCTION
01.20 C (UNLESS OTHERWISE SPECIFIED, DATA WILL BE STORED IN HDAT.FD)
01.30 C INPUT: BASELINE, H2O ABS AT 1869CM-1, N2H4 ABS AT 1605CM-1.
01.40 C OUTPUT: H2O AND N2H4 CONCENTRATION(PPM).
01.50 C TO END DATA INPUT TYPE 99999 FOR FILE ID.

02.10 S A=FOUT(27)+FOUT(12)
02.30 A !"DO YOU WANT TO SPECIFY NAME OF OUTPUT FILE? (Y OR N)"Q
02.50 I (Q-000N)2.7,3.1,2.7
02.70 I (Q-000Y)2.3,2.8,2.3
02.80 T !!!"TYPE 0 0 FILENAME, RETURN, THEN GO AT 3.1"!
02.90 M 5.1

03.10 T !!!"TYPE DATE OF RUN MM/DD/YY "
03.20 F I=1,8;S D(I)=FIN()
03.30 O O INTERM;O O TTY:,E;F I=1,8;D 3.4
03.35 G 3.5
03.40 O R O;S A=FOUT(D(I))
03.50 O O TTY:,E
03.60 A !!!"INITIAL FILE ID: "ID
03.65 A !!!"INITIAL BASELINE: "B
03.67 A !!!"INITIAL H2O ABSORBANCE: "W
03.69 A !!!"INITIAL N2H4 ABSORBANCE: "H;S T=0
03.70 O R O;T ID,T,B,W,H;O O TTY:,E;S CNT=1
03.80 S A=FOUT(27)+FOUT(12);T !!!"ENTER DATA"!
03.90 T !!!"SPECTRAL",:15"TIME",:26"TIME",:36"BASE-",:47"H20",:56"N2H4"
03.93 T !!!"FILE ID",:15"START",:26"END",:36"LINE",:47"ABS",:56"ABS"!

04.10 A !ID;I (ID-99999)4.2,4.9,4.2
04.20 A :15,T1,:26,T2,:36,B,:47,W,:56,H
04.30 S CNT=CNT+1;S T=(T1+T2)/2
04.40 O R O;T ID,T,B,W,H
04.50 O O TTY:,E;G 4.1
04.90 O C

05.10 O O HDAT
05.20 O I INTERM;O O TTY:,E;O I TTY:,E
05.30 F I=1,8;D 5.4
05.35 G 5.5
05.40 O R I;S D(I)=FIN();O R O;S A=FOUT(D(I))
05.50 O I TTY:,E;O O TTY:,E;S A=FOUT(27)+FOUT(12)
05.60 T !!!"RUN OF ";F I=1,8;S A=FOUT(D(I))
05.70 T !!!"SPECTRL",:25,"H20",:34,"N2H4"
05.80 T !!!"FILE ID",:15,"TIME",:25,"PPM",:34,"PPM"!
```

THIS PAGE IS BEST QUALITY PRACTICABLE
FROM COPY FURNISHED TO DDC

```
06.10 O R I;A ID,T,B,W,H;O I TTY:,E
06.20 S CNT=CNT-1;S W=W-B;S H=H-B
06.30 S WC=.061+.223*W+.003*W*W;S HC=H-WC
06.40 S WPPM=17.56*(W-1.43);S HPPM=5.*HC
06.50 T !,%4.0,1D,:13,T
06.60 T %4.1,:23,WPPM,:32,HPPM
06.65 O R O;T ID,T,WPPM,HPPM;O O TTY:,E
06.70 I (CNT) 6.1,6.9,6.1
06.90 O C
06.99 G 9.9

09.90 Q
*
```

THIS PAGE IS BEST QUALITY PRACTICABLE
FROM COPY FURNISHED TO DDC

C-PS/8 FOCAL, 1971

```
01.10 C HYDLST--LIST OUTPUT FILE FROM HYDRAZ
01.50 T !"SPECIFY NAME OF DATA FILE TO BE PRINTED."
01.52 T !"    TYPE O I FILENAME, RETURN, THEN GO AT 2.1",!!
01.55 M 2.1

02.10 O I HDAT
02.20 O I TTY:,E
02.30 F I=1,8; D 2.4
02.35 G 2.5
02.40 O R I; S D(I)=FIN()
02.50 O I TTY:,E; S A=FOUT(27)+FOUT(12)
02.60 T !"RUN OF "; F I=1,8; S A=FOUT(D(I))
02.70 T !!!"SPECTRAL" :25,"H2O" :34,"N2H4"
02.80 T !!!"FILE ID" :15,"TIME" :25,"PPM" :34,"PPM"

03.10 O R I; A ID,T,WPPM,HPPM
03.20 O I TTY:,E; T !
03.30 T %4.0 ID,:13 T
03.40 T %4.1 :23 WPPM,:32 HPPM
03.50 G 3.1
03.93 T !!!"FILE ID", :15 "START",:26 "END",:36 "LINE",:47 "ABS",:56 "ABS"
*
```